NANO LETTERS

Letter

In Vitro and In Vivo Nonlinear Optical Imaging of Silicon Nanowires

Yookyung Jung, Ling Tong, Asama Tanaudommongkon, Ji-Xin Cheng, and Chen Yang

Nano Lett., **Article ASAP** • Publication Date (Web): 06 May 2009

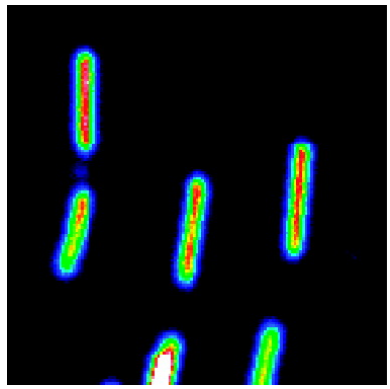

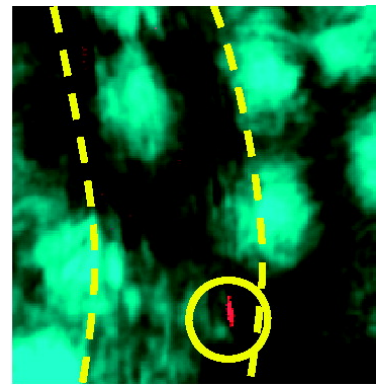

More About This Article

Additional resources and features associated with this article are available within the HTML version:

- Supporting Information
- Access to high resolution figures
- Links to articles and content related to this article
- Copyright permission to reproduce figures and/or text from this article

View the Full Text HTML

Nano Letters is published by the American Chemical Society. 1155 Sixteenth Street N.W., Washington, DC 20036

NANO LETTERS

XXXX
Vol. xx, No. x
-

In Vitro and In Vivo Nonlinear Optical Imaging of Silicon Nanowires

Yookyung Jung,[†,||] Ling Tong,[‡,||] Asama Tanaudommongkon,[‡] Ji-Xin Cheng,[‡,§] and Chen Yang*[,†,‡]

Department of Physics, Department of Chemistry, Weldon School of Biomedical Engineering, Purdue University, West Lafayette, Indiana

Received April 9, 2009

ABSTRACT

Understanding of cellular interactions with a nanostructure requires tracking directly the nanostructure. Current investigation is challenged by the lack of a strong, intrinsic signal from the nanostructure. We demonstrate intensive four-wave mixing and third-harmonic generation signals from dimension-controllable silicon nanowires as small as 5 nm in diameter. The nonlinear optical signals observed from the nanowires are highly photostable with an intensity level of 10 times larger than that observed from silver nanoparticles of comparable sizes. This intrinsic optical signal enabled intravital imaging of nanowires circulating in the peripheral blood of a mouse and mapping of nanowires accumulated in the liver and spleen, opening up further opportunities to investigate in vivo cellular response to nanomaterials as a function of size, aspect ratio, and surface chemistry.

The translation of nanomedicine to a clinical setting has been slowed down due to limited fundamental understanding of the interactions between nanomaterials and biological cells.[1] Current study of cellular interactions with a nanomaterial is challenged by the lack of a strong intrinsic signal from a dimension-controllable nanostructure. Although routinely used as labels for visualization of nanosized drug carriers, such as liposomes, polymer particles, and copolymer micelles, fluorescent agents often suffer from photobleaching. The interpretation of fluorescence data could be further complicated due to dissociation of probes from the objects to be studied. For example, recent research revealed an unexpected release of lipophilic dyes from copolymer micelles[2,3] and poly(lactic-co-glycolic acid) nanoparticles[4] to lipid-rich structures during cellular uptake or blood circulation. Intrinsic near-infrared fluorescence[5,6] and spontaneous Raman scattering[7] have been used to track carbon nanotubes in live cells and live animals, where the lengths of nanotubes were limited to several hundred nanometers. An intrinsic multiphoton luminescence[8] has been used to visualize low-aspect-ratio gold nanorods and nanoshells in live cells[9] and implanted tumors[10] while more than 95% of the excitation energy is actually converted into heat, causing effective phototoxicity to cells.[9,11] Therefore, in order to decipher cellular response to nanostructures, nanosystems with precise controls of size, shape, and surface chemistry and an intense and intrinsic optical signal with low damage potential are desired. Silicon nanowires (SiNWs) have unparalleled dimension-control properties with diameters controlled from ~3 up to 100 nm,[12,13] and lengths from a few hundred nanometers to tens of micrometers.[14] In this paper, we report strong and stable third-order nonlinear optical (NLO) signals, including four-wave mixing (FWM) and third-harmonic generation (THG), from silicon nanowires (SiNWs) of diameters as small as 5 nm. We further employ such signals to monitor SiNWs circulating in the peripheral blood of a live mouse and to map the organ distribution of systemically administrated SiNWs.

SiNWs were synthesized by chemical vapor deposition of silane using 40, 20, and 5 nm Au colloids (Ted Pella) as catalysts.[12] For in vitro imaging, nanowires were transferred onto coverslips through gentle friction between the as-grown nanowire substrate and the coverslip, which also aligned nanowires in a relatively parallel fashion. FWM and THG images of SiNWs were acquired on a multimodal NLO microscope with configurations as follows. A femtosecond laser (Mai tai, Spectra-Physics, Fremont, CA) generated 130 fs pulse at a repetition rate of 80 MHz. Eighty percent of the Mai Tai output at 790 nm was used to pump an optical parametric oscillator (OPO) (Spectra-Physics, Fremont, CA) generating a signal beam at 1290 nm and an idler beam at 2036 nm. The frequency of the idler beam was doubled to 1018 nm by a PPLN crystal. The 1018 nm beam was used as the Stokes beam. The other 20% of the Mai Tai beam was used as the pump beam. These two beams were

* To whom correspondence should be addressed. E-mail: yang@purdue.edu.
† Department of Physics.
‡ Department of Chemistry.
§ Weldon School of Biomedical Engineering.
|| These authors contributed equally to this work.

10.1021/nl901143p CCC: $40.75

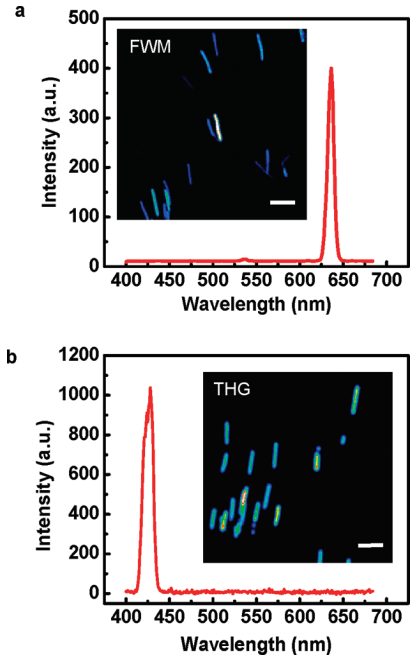

Figure 1. Imaging NWs with NLO signals. (a) FWM image and spectrum of SiNWs. The pump and Stokes laser power at the sample were 0.8 and 1.2 mW, respectively. (b) THG image and spectrum of SiNWs. The 1290 nm laser power at the sample was 8.6 mW. All images and spectra were recorded in 0.5 s. Scale bars, 2 μm.

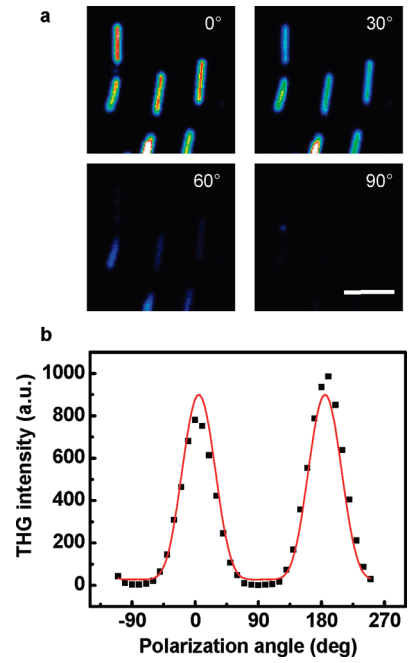

Figure 2. Polarization dependence of THG intensity from SiNWs. (a) THG images of aligned SiNWs under the excitation polarization 0° (upper left), 30° (upper right), 60° (lower left), and 90° (lower right) with respect to the nanowire axis. Scale bar, 2 μm. (b) Measured THG intensity (solid squares) as a function of excitation polarization angle relative to the nanowire axis. Red curve, a least-squares fitting by $\cos^6 \theta$.

collinearly combined with the Stokes beam passing through a delay line. The combined beams were sent into a FV1000 laser-scanning microscope (Olympus America Inc., PA) and focused into a sample using a 60× water objective lens with a numerical aperture of 1.2. The backward NLO signal was separated from the excitation laser by a dichroic mirror and detected by an external photomultiplier tube after passing through a bandpass filter (430/40 nm for THG, 650/40 nm for FWM). Emission spectra were recorded with the internal spectral detector of the microscope.

SiNWs of 40 nm diameters synthesized exhibit strong emissions in both FWM and THG images (Figure 1a,b, insets). The FWM and THG emission spectra recorded from individual nanowires in the 400−680 nm region display a peak at 645 nm (Figure 1a) and at 428 nm (Figure 1b), respectively. These peak positions are in agreement with the emission wavelengths of FWM, 645 nm, generated by collinearly combined pump field (790 nm) and Stokes field (1018 nm), and THG, 430 nm, produced by 1290 nm excitation, confirming that the contrast in the images (Figure 1a,b, insets) arises from FWM and THG, respectively.

It is evident that the FWM signal is not resonant with the Raman shift of approximately 520 cm^{-1} observed previously in SiNWs.[15−17] This vibrationally nonresonant yet strong emission suggests the possibility of further enhancing the FWM signal level by tuning the pump and/or Stokes laser wavelengths. The intensive FWM and THG emission from SiNWs could be attributed to the large third-order susceptibility of crystal silicon, which is approximately 1−2 orders of magnitude higher than that of other materials such as crystal CdS, TiO_2, and Au.[18] Notably, second harmonic generation (SHG) signals in nanowires have been reported.[19] Strong SHG response from potassium niobate ($KNbO_3$) nanowires partially resulted from its large nonlinear optical coefficients enabled a nanometric light source when a single $KNbO_3$ nanowire was optically trapped.[20] In our case, the intensive intrinsic THG signals enabled visualization of individual SiNWs with diameter as small as 5 nm (Supporting Information, Figure S1) and were employed for real-time imaging in vivo. Additionally, the lateral and depth full-width-at-half-maximum (fwhm) of the FWM signal measured on a single nanowire were measured to be 0.30 and 1.43 μm (Supporting Information, Figure S2), respectively. Such three-dimensional (3D) spatial resolution allowed us to monitor individual SiNWs grown on a quartz substrate (Supporting Information, Figure S3) or dispersed in a 3D collagen scaffold (Supporting Information, Figure S4).

THG images of aligned SiNWs were recorded while rotating the polarization of the excitation laser to 0, 30, 60, and 90° with respect to the nanowire axis (Figure 2a). The results show that the THG intensity was maximized when the polarization of excitation was parallel with the nanowire axis and almost depleted when the polarization of excitation was perpendicular to the nanowire axis.[19]

As shown in Figure 2b, the THG intensity measured on a representative nanowire exhibits a periodic dependence on the angle θ. This periodic polarization dependence could be modeled by treating the nanowire as an infinite dielectric cylinder similarly as that in the previous photoluminescence study of nanowires.[21] According to this model, the perpendicularly polarized electric field inside the cylinder E_{in} is attenuated to 75% of the excited field E_e based on E_{in} =

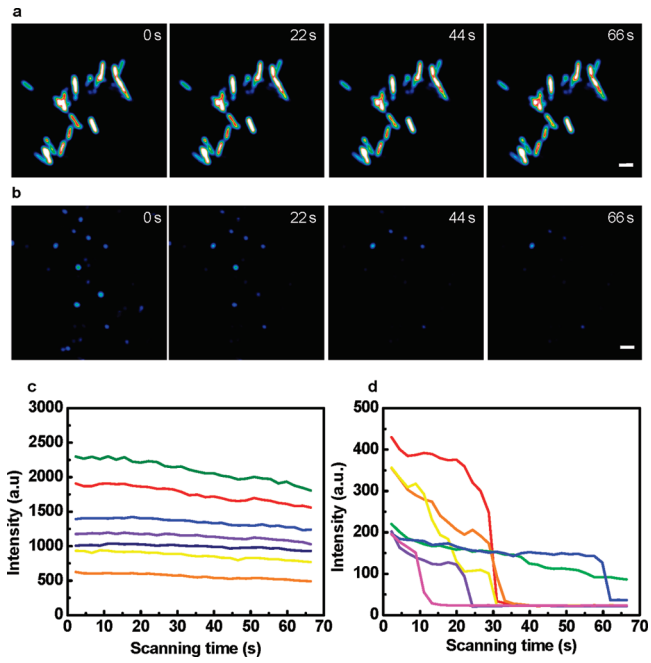

Figure 3. THG intensity and photostability of SiNWs and silver NPs. (a) THG images of silicon NWs recorded at different scanning time. (b) THG images of silver NPs recorded at different scanning time. The scanning time is indicated in each image. Scale bars, 2 μm. (c) THG intensity of seven representative SiNWs as a function of the scanning time. (d) THG intensity of seven representative silver NPs as a function of the scanning time. The THG signals were produced by the 1290 nm beam with 8.6 mW at the samples.

$(2\varepsilon_0)/(\varepsilon_0 + \varepsilon)E_e$, where ε and ε_0 are the dielectric constants of silicon and vacuum.[22] As a result, the signal intensity arising from the perpendicular polarization is much smaller than that from parallel polarization. Distinguished from the previous $\cos^2\theta$ dependence found in one-photon photoluminescence and Raman scattering of nanowires,[21,23] the corresponding THG intensity is expected to show a $\cos^6\theta$ dependence on the polarization of excitation, as the THG field is proportional to the cube of the excitation field. This $\cos^6\theta$ relationship is confirmed by the least-squares fitting (red curve) shown in Figure 2b.

To evaluate its potential as a valid NLO imaging agent, we compared the THG signal intensity and photostability of single SiNWs with those of silver nanoparticles (NPs), one of the strongest THG emitters studied previously.[24,25] We continuously scanned 40-nm diameter SiNWs and 60-nm diameter silver NPs for 70 s with 8.6 mW of the 1290 nm beam at the sample. A strong THG intensity is expected from silver NPs because the THG wavelength generated (430 nm) is near the surface plasmon resonance wavelength of these NPs. THG images acquired at the scanning time of 0, 22, 44, and 66 s show that the THG intensity of the SiNWs remain consistent over the time (Figure 3a). In comparison, THG signals from the silver NPs quenched quickly and few signals from silver NPs were observed after 60 s (Figure 3b). The rapid decrease of the THG intensity is possibly due to melting of the NPs by the ultrafast pulses. For quantitative analysis of the intensity levels, the THG intensities of seven SiNWs and seven silver NPs versus the scanning time are plotted in Figure 3c,d, respectively. Under the same condition of excitation, the THG intensity at the beginning of scanning ranged from 600 to 2300 au for the SiNWs and from 200 to 450 au for the silver NPs. The intensity difference between

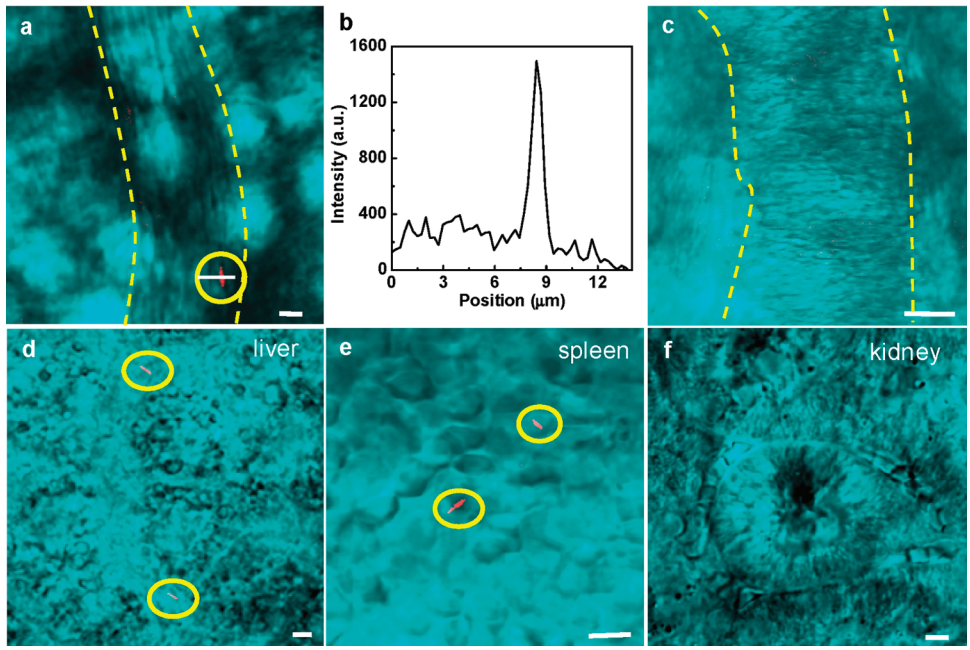

Figure 4. In vivo FWM images of SiNWs. (a) FWM image (red) of the peripheral blood of a living mouse taken at 20 min post injection of PEGylated SiNW PBS solution. Yellow dashed lines mark the blood vessel. The white solid line indicates the scan line for the intensity profile showed in b. (b) FWM intensity profile from the linescan along the flowing SiNW. (c) FWM image of the peripheral blood of a living mouse taken post injection of PBS. (d−f) FWM images of SiNWs (red) deposited in liver (d), spleen (e), and kidney (f) explanted at 1 h post injection. All FWM images are superimposed with transmission images (cyan) taken simultaneously. The SiNWs were highlighted by yellow circles. Scale bars, 5 μm.

individual nanowires is caused by the orientation variation. For silver NPs, the intensity distribution can be due to various aggregations. This comparison shows that the SiNWs produced approximately ten times stronger THG than the silver NPs. Results above demonstrate that SiNWs can be rendered as an extremely intensive and stable NLO imaging agent.

The potential of SiNWs in intravital imaging were demonstrated for the first time by real time imaging of polyethylene glycol (PEG)-modified SiNWs circulating in the blood vessels inside a mouse earlobe. PEGylation has been found to be able to prolong the blood circulation time for other nanosystems, such as liposomes,[26] Au nanorods,[27] and carbon nanotubes,[28] thus modification of SiNWs with PEG are expected to promote circulations of SiNWs in the blood to facilitate the imaging. We introduced 100 μL of phosphate buffered saline (PBS) containing 0.1−1 pM PEGylated SiNWs[29] of ∼5 μm in length to an anesthetized BALB/c mouse through tail vein injection. The laser beam was focused on the ear lobe using a 40× water-immersion objective. The laser power at the sample was 23 mW for the pump beam and 2 mW for the Stokes beam. The backward FWM signal was detected by an external photomultiplier tube with bandpass filters of 645/40 nm. The blood vessel and surrounding tissues were visualized by transmission illumination and the circulating SiNWs were monitored by epi-detected FWM simultaneously with scanning rate of 2 μs/pixel and 256 × 256 pixels/frame (Supporting Information, video 1). One frame is shown in Figure 4a. The FWM signal presents an elongated shape with approximately 5 μm in the elongated direction, which is consistent with the length of SiNWs synthesized. Additionally, the FWM intensity profile across the flowing SiNW (Figure 4b) shows a peak intensity of 1500 au, which is 5 times larger than the background (∼300 au) from the blood. Such FWM signal was not detected in the control mouse injected with 100 μL pure PBS (Figure 4c). After 30 min post injection, we could no longer detect any FWM signals from the SiNWs in the bloodstream. Compared to blood circulation time ranging from 1.5 to 15 h observed for single carbon nanotubes with various PEGylations,[7] the shorter circulation time of SiNW could be due to the shorter PEG chain used and/or dimension difference between SiNWs and carbon nanotubes. Further systematic investigation will be carried out to address these issues.

Using the FWM signals, we further studied the distribution of SiNWs in the organs explanted at 1 h post injection. To prepare explanted organ tissues, the mouse was euthanatized at 1 h after intravenous injection of SiNWs. Organs including liver, spleen and kidney were explanted, fixed in 4% formalin solution to preserve the tissue architecture, and cut into small pieces by blade for imaging. The laser beams were focused onto the sample using a 60× water-immersion objective with a laser power of 10 mW for pump beam and 3 mW for Stokes beam at the sample. FMW images superimposed with transmission images taken simultaneously show that the SiNWs appearing wire shapes were found in both liver (Figure 4d) and spleen (Figure 4e) tissues. The depth-resolved distributions can be found in the Supporting Information, video 2. No SiNWs were observed in the kidney (Figure 4f). These results suggest that most of the injected SiNWs were captured by the reticuloendothelial system but not filtered through kidney. It is conceivable that the SiNWs were captured by the macrophages while circulating through the liver and spleen.

In summary, we have demonstrated that SiNWs exhibit intensive FWM and THG emissions with a $\cos^6 \theta$ polarization dependence. These properties open up exciting opportunities for using SiNWs as a novel in vivo imaging agent offering intrinsic 3D spatial resolution, high photostability, and orientation information. With the advantages of highly controllable dimensions, versatile surface chemistry, and an intensive intrinsic NLO signals, SiNWs provide an exciting nanobio system for investigating the cellular interaction with one-dimension nanomaterials.

Acknowledgment. The work was supported by start-up funds from Purdue University, NSF Grant CBET 0828832, and American Heart Association predoctoral fellowship for Ling Tong.

Supporting Information Available: Depth-resolved FWM images of SiNWs spread on a coverslip (Figure S1). Reconstructed 3D THG image of as-grown 5 nm SiNWs on a quartz substrate (Figure S2). SiNWs embedded in a collagen gel served as a tissue scaffold (Figure S3). THG images of SiNWs with diameters of 40, 20, and 5 nm (Figure S4). In vivo FWM imaging of SiNWs circulating in a blood vessel recorded at 15 min after injection (Supporting Video 1). Depth-resolved FWM imaging of SiNWs deposited in spleen explanted at 1 h postinjection (Supporting Video 2). This material is available free of charge via the Internet at http://pubs.acs.org.

References

(1) Sanhai, W. R.; Sakamoto, J. H.; Canady, R.; Ferrari, M. *Nat. Nanotechnol.* **2008**, *3*, 242–244.
(2) Chen, H.; Kim, S.; Li, L.; Wang, S.; Park, K.; Cheng, J. X. *Proc. Natl. Acad. Sci. U.S.A.* **2008**, *105*, 6596–6601.
(3) Chen, H.; Kim, S.; He, W.; Wang, H.; Low, P. S.; Park, K.; Cheng, J. X. *Langmuir* **2008**, *24*, 5213–17.
(4) Xu, P.; Gullotti, E.; Tong, L.; Highley, C. B.; Errabelli, D. R.; Hasan, T.; Cheng, J. X.; Kohane, D. S.; Yeo, Y. *Mol. Pharm.* **2009**, *6*, 190–201.
(5) Cherukuri, P.; Gannon, C. J.; Leeuw, T. K.; Schmidt, H. K.; Smalley, R. E.; Curley, S. A.; Weisman, R. B. *Proc. Natl. Acad. Sci. U.S.A.* **2006**, *103*, 18882–18886.
(6) Jin, H.; Heller, D. A.; Strano, M. S. *Nano. Lett.* **2008**, *8* (6), 1577–85.
(7) Liu, Z.; Davis, C.; Cai, W.; He, L.; Chen, X.; Dai, H. *Proc. Natl. Acad. Sci. U.S.A.* **2008**, *105* (5), 1410.
(8) Wang, H.; Huff, T. B.; Zweifel, D. A.; He, W.; Low, P. S.; Wei, A.; Cheng, J.-X. *Proc. Natl. Acad. Sci. U.S.A.* **2005**, *102*, 15752–15756.
(9) Tong, L.; Zhao, Y.; Huff, T. B.; Hansen, M. N.; Wei, A.; Cheng, J. X. *Adv. Mater.* **2007**, *19*, 3136–41.
(10) Park, J.; Estrada, A.; Sharp, K.; Sang, K.; Schwartz, J. A.; Smith, D. K.; Coleman, C.; Payne, J. D.; Korgel, B. A.; Dunn, A. K.; Tunnell, J. W. *Opt. Express* **2008**, *16* (3), 1590–1599.
(11) Huang, X.; El-Sayed, I. H., Q., W.; El-Sayed, M. A. *J. Am. Chem. Soc.* **2006**, *128*, 2115–2120.
(12) Cui, Y.; Lauhon, L.; Gudiksen, M.; Wang, J.; Lieber, C. *Appl. Phys. Lett.* **2001**, *78*, 2214–2216.
(13) Wu, Y.; Cui, Y.; Huynh, L.; Barrelet, C. J.; Bell, D. C.; Lieber, C. M. *Nano Lett.* **2004**, *4* (3), 433–436.
(14) Yang, C.; Zhong, Z.; Lieber, C. M. *Science* **2005**, *310*, 1304.

(15) Zhang, Y. F.; Tang, Y. H.; Wang, N.; Yu, D. P.; Lee, C. S.; Bello, I.; Lee, S. T. *Appl. Phys. Lett.* **1998**, *72*, 1835–1837.
(16) Li, B.; Yu, D.; Zhang, S.-L. *Phys. Rev. B* **1999**, *59*, 1645–1648.
(17) Wang, R.-p.; Zhou, G.-w.; Liu, Y.-l.; Pan, S.-h.; Zhang, H.-z.; Yu, D.-p.; Zhang, Z. *Phys. Rev. B* **2000**, *61*, 16827–16832.
(18) Boyd, R. W. *Nonlinear Optics*, 2nd ed.; Academic Press: Boston, 2003.
(19) Johnson, J. C.; Yan, H.; Schaller, R. D.; Petersen, P. B.; Yang, P.; Saykally, R. J. *Nano Lett.* **2002**, *2* (4), 279–283.
(20) Nakayama, Y.; Pauzauskie, P. J.; Radenovic, A.; Onorato, R. M.; Saykally, R. J.; Liphardt, J.; Yang, P. *Nature* **2007**, *447*, 1098–1102.
(21) Wang, J.; Gudiksen, M.; Duan, X.; Cui, Y.; Lieber, C. *Science* **2001**, *294*, 1455–1457.
(22) Landau, L. D.; Lifshitz, E. M.; Pitaevskii, L. P., *Electrodynamics of Continuous Media*, 2nd ed.; Butterworth-Heinemann: Oxford, 1984.
(23) Xiong, Q.; Chen, G.; Gutierrez, H. R.; Eklund, P. C. *Appl. Phys. A* **2006**, *85*, 299–305.
(24) Tai, S.-P.; Wu, Y.; Shieh, D.-B.; Chen, L.-J.; Lin, K.-J.; Yu, C.-H.; Chu, S.-W.; Chang, C.-H.; Shi, X.-Y.; Wen, Y.-C.; Lin, K.-H.; Liu, T.-M.; Sun, C.-K. *Adv. Mater.* **2007**, *19* (24), 4520–4523.
(25) Liu, T.-M.; Tai, S.-P.; Yu, C.-H.; Wen, Y.-C.; Chu, S.-W.; Chen, L.-J.; Prasad, M. R.; Lin, K.-J.; Sun, C.-K. *Appl. Phys. Lett.* **2006**, *89*, 043122.
(26) Lasic, D. D.; Needham, D. *Chem. Rev.* **1995**, *95* (8), 2601–2628.
(27) Niidome, T.; Yamagata, M.; Okamoto, Y.; Akiyama, Y.; Takahashi, H.; Kawano, T.; Katayama, Y.; Niidome, Y. *J. Controlled Release* **2006**, *114* (3), 343–347.
(28) Liu, Z.; Cai, W.; He, L.; Nakayama, N.; Chen, K.; Sun, X.; Chen, X.; Dai, H. *Nat. Nanotechnol.* **2007**, *2* (1), 47–52.
(29) To prepare PEGylated nanowires, SiNW growth substrates were first modified with 1% v/v 3-(trimethoxysilyl)propyl aldehyde in ethanol for 0.5 h, followed with reaction with 0.1% PEG (MW = 900 Da) in the presence of sodium cyanoborohydride for 24 h. The PEGylated nanowires were removed from the growth substrate by sonication into a phosphate buffered saline (PBS). The concentration of a nanowire solution was estimated by measured weight difference of the unmodified as-grown substrate before and after sonication.

NL901143P